Organic Ferroelectrics

DOI: 10.1002/anie.200700407

A Supramolecular Ferroelectric Realized by Collective Proton Transfer**

Sachio Horiuchi, Reiji Kumai, and Yoshinori Tokura*

Hydrogen bonds, which bind two or more electronegative atoms as X–H···Y, have been utilized to construct molecular assemblies in crystal engineering, supramolecular chemistry, and molecular recognition.[1] The dynamics of proton transfer through hydrogen bonds has attracted extensive interest, because of the crucial role played by proton transfer in many chemical reactions and biological functions, and also because of its potentially diverse applications in electronic and optical devices.[2] In organic molecular solids, proton transfer is often accompanied by a tautomerism of the π-electron configuration, which can be associated with novel functionalities; transformations between the keto and enol forms of molecules have been reported to produce a reversible color change[3] or a dipole inversion.[4] Importantly, such a motion of protons can be correlated even through intermolecular space, if each molecule is restricted in its total number of protons, as is typically found in the case of ice. Squaric acid ($H_2C_4O_4$)[5] provides a good example of this constraint called the "ice rule": cooperative proton transfer over the short O···O bonds (2.55 Å) can reverse the polarity of the hydrogen-bonded molecular sheets. As a consequence, a high dielectric permittivity emerges near the order–disorder phase transition. As in this example, the three-dimensional arrangement of polar molecules is usually antiparallel (antiferroelectric), canceling out the net electric polarization. If the mobile protons were ordered into a polar lattice, they would generate a spontaneous polarization, and their motion could be controlled with an external electric field, as a ferroelectric.

Herein, we report the first organic system that exhibits ferroelectricity induced by a cooperative intermolecular proton transfer. KH_2PO_4 (KDP) is a representative inorganic ferroelectric, in which the electric polarization is reversed by an electric field through a site-to-site proton transfer over very short O···O bonds (2.50 Å) between the PO_4^{2-} ions.[6] Molecular analogues of KDP are still undeveloped, except for an organic–inorganic hybrid, the salt $[dabcoH]^+[ReO_4]^-$ (dabco = diazabicyclo[2.2.2]octane).[7]

To design genuinely organic ferroelectrics, we have exploited a strongly hydrogen-bonded acid–base system, because some such compounds are known to exhibit novel thermally induced proton migration.[8] The combination of acids and bases with similar proton affinities guarantees that the protons of the hydrogen bonds can easily attach to both molecules.[9] Cocrystals of 2,5-dihydroxy-*p*-benzoquinones as the acid and pyridine derivatives as the base (Scheme 1) have

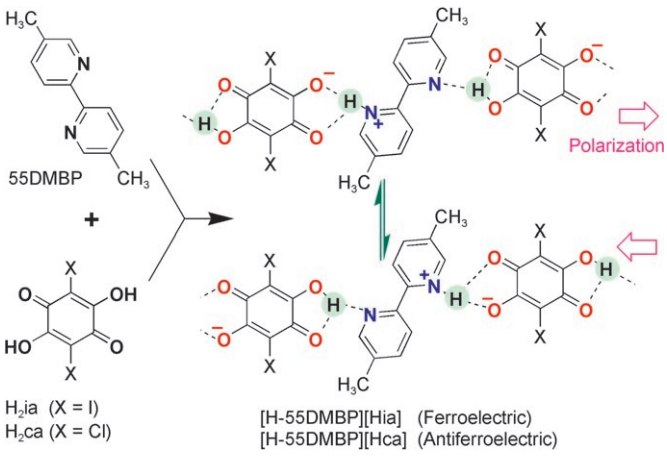

Scheme 1. The formation of polar chains of alternating acid and base molecules through hydrogen bonding (dashed lines) and the reversal of their polarization through a cooperative transfer of protons (green circles).

recently been tested to fulfill this requirement. For example, it was demonstrated that chloranilic acid (H_2ca; Scheme 1, X = Cl) and bromanilic acid (X = Br) produce ferroelectric adducts with phenazine (Phz).[10] In these adducts, however, there is no apparent site-to-site proton transfer and the ferroelectricity is, rather, classified as displacive, as is found for the $BaTiO_3$ or $PbTiO_3$ family. On the other hand, an antiferroelectric phase transition with proton ordering was realized in a proton-transferred monovalent salt of H_2ca with a stronger base, 5,5′-dimethyl-2,2′-bipyridine (55DMBP; Scheme 1).[11] The new ferroelectric presented herein is derived from the iodine analogue of H_2ca, iodanilic acid (H_2ia; Scheme 1, X = I), and 55DMBP. This compound is also a proton-transferred 1:1 salt, as formulated by [H-

[*] Dr. S. Horiuchi, Dr. R. Kumai, Prof. Y. Tokura
Correlated Electron Research Center (CERC), National Institute of Advanced Industrial Science and Technology (AIST)
Tsukuba, Ibaraki, 305–8562 (Japan)
Fax: (+81) 29-861-2945
E-mail: s-horiuchi@aist.go.jp
Prof. Y. Tokura
Department of Applied Physics, University of Tokyo
Hongo, Bunkyo-ku, Tokyo, 113-8656 (Japan)
and
Tokura Multiferroics Project, ERATO, JST
c/o AIST, Tsukuba, Ibaraki, 305-8562 (Japan)

[**] The authors thank F. Ishii, T. Hasegawa, Y. Takahashi, and H. Sawa for enlightening discussions. This study was partly supported by a Grant-in-Aid for Scientific Research (no. 18750133) from the Ministry of Education, Culture, Sports, Science and Technology of Japan.

Supporting information for this article is available on the WWW under http://www.angewandte.org or from the author.

55DMBP]$^+$[Hia]$^-$. The cocrystals were prepared by the slow evaporation of a methanol solution of H_2ia and 55DMBP. By using CH_3OD as the solvent, the acidic protons could be readily deuterated to give [D-55DMBP][Dia].

The crystal structure of [H-55DMBP][Hia] was determined by synchrotron X-ray diffraction experiments on a single crystal at 50 K (Figure 1).[12] The triclinic unit cell

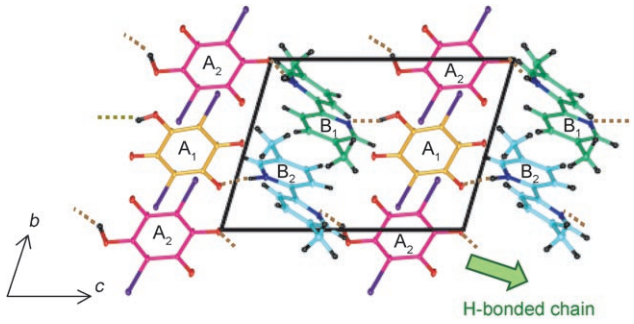

Figure 1. The crystal structure of [H-55DMBP][Hia] at 50 K viewed along the *a* axis. The acid (A_1 and A_2) and base (B_1 and B_2) molecules are connected into chains by hydrogen bonds (dashed lines). The direction of propagation of the chains is indicated by the green arrow. C yellow (A_1), pink (A_2), green (B_1), or blue (B_2); H black, N blue, O red.

(space group *P*1) comprises two acid molecules (A_1 and A_2) and two base molecules (B_1 and B_2). The acid and base molecules alternate in hydrogen-bonded chains along the [0$\bar{1}$2] direction and are π-stacked in individual columns parallel to the *b* axis. The acid molecules are almost planar, whereas the base molecules adopt a twisted *trans* configuration with dihedral angles of 19.5–20.9° between the pyridyl rings. All the hydrogen bonds have notably short distances (O···N 2.61–2.70 Å, N^+···O^- 2.54–2.55 Å).

The dielectric constant ε of [H-55DMBP][Hia] at ambient pressure is very large ($\varepsilon = 800$) and strongly temperature-dependent near room temperature (Figure 2a). A phase transition is apparent by the sharp peak in the dielectric-constant curve, which occurs at $T_c = 268$ and 270 K on cooling and heating, respectively, showing a clear thermal hysteresis. Curie–Weiss behavior obeying $\varepsilon = C/(T-\theta)$ is characteristic of ferroelectricity. The Weiss temperature θ deduced from the linear $1/\varepsilon$ versus T relationship for the paraelectric phase is approximately 17 K lower than the Curie temperature T_c. Both the detection of thermal hysteresis and the disagreement between T_c and θ indicate the first-order nature of the phase transition. Importantly, deuteration of the hydrogen bonds significantly raises the phase-transition temperature to far above room temperature ($T_c = 335$ K, $\Delta T_c = 67$ K). These T_c values are much higher than those of the conventional KDP family.[13] Note that the dielectric response is highly anisotropic. Large ε values were obtained only with the ac electric field applied parallel to the crystal *c* axis, which is slightly inclined to the hydrogen-bonding direction. Measurements with the field applied parallel to the *a** axis or to the *b* axis yielded much smaller dielectric constants ($\varepsilon \leq 10$). The one-dimensional character and the significant hydrogen/

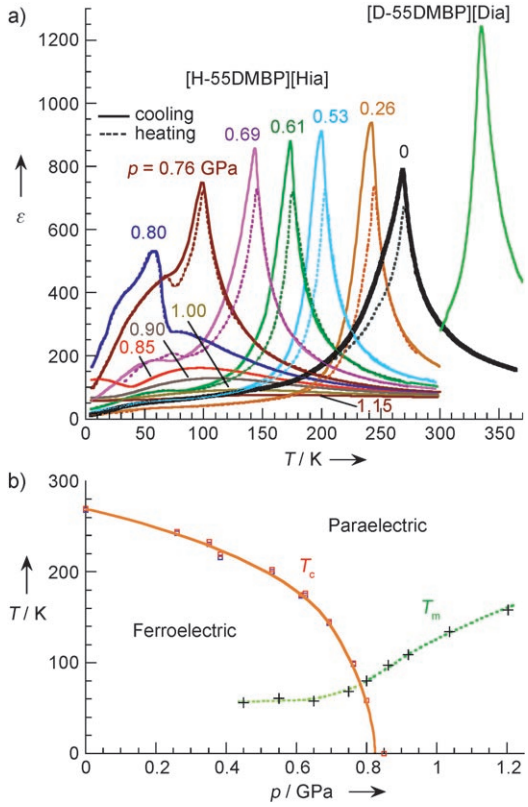

Figure 2. a) Temperature dependence of the dielectric constant ε of [H-55DMBP][Hia] at various pressures and of [D-55DMBP][Dia] at ambient pressure. The measurement was made in an electric field of 100 kHz applied along the *c* axis. b) Pressure dependence of the ferroelectric transition temperature T_c and the temperature of the anomaly T_m (see text for details) of [H-55DMBP][Hia].

deuterium isotope effect manifest that the hydrogen-bonded chains play a central role in producing the ferroelectricity.

Besides the Curie–Weiss behavior of the dielectric constant, ferroelectricity is further evident from the polarization hysteresis loops measured below the phase-transition temperature. Figure 3 shows the thermal evolution of the electric polarization *P* with an ac electric field *E* of triangle waveform applied parallel to the crystal *c* axis. At temperatures far below T_c, crystals of [H-55DMBP][Hia] and [D-55DMBP]-[Dia] show saturated polarizations P_s of 1.2 and 1.7 μC cm^{-2}, respectively, as estimated by extrapolation of the *P* versus *E* curves. Their remnant polarizations P_r measured with the field *E* sweeping back to zero are 0.9 and 1.5 μC cm^{-2}, respectively. These values are very large compared with those of other organic ferroelectrics, and are even larger than the maximum known values of the Phz-based cocrystals ($P_r = 0.7$–0.8 μC cm^{-2}).[10] Furthermore, the coercive field E_c is relatively small ($E_c \approx 2$ kV cm^{-1}); hence, a hysteresis curve was easily measured at ambient pressure for the room-temperature ferroelectric [D-55DMBP][Dia].

One feature of ferroelectrics based on proton dynamics is that the phase transition is very sensitive to the hydrostatic pressure, as shown by the ε versus *T* curves in Figure 2a. The applied pressures *p* were corrected by considering the effect

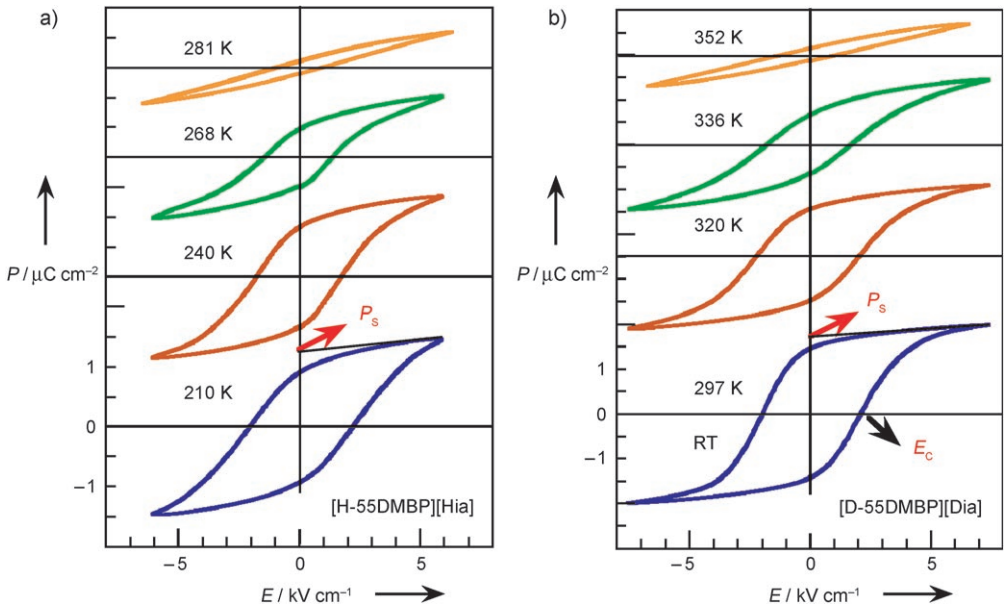

Figure 3. Hysteresis loops of the electric polarization P versus the electric field E at various temperatures for a) [H-55DMBP][Hia] and b) [D-55DMBP][Dia].

of the thermal contraction at T_c of the pressure-transmitting oil (Daphne 7373, Idemitsu) in the clamp-type high-pressure cell.[14] The transition temperature decreases smoothly with pressure, as is typical of the KDP family and the displacive-type ferroelectrics.[15] As evidenced by the detection of thermal hysteresis, the first-order nature of the phase transition persists to pressures up to at least 0.75 GPa. The nonlinear drop in T_c becomes steeper approaching $p_c \approx 0.8$ GPa, at which the phase transition suddenly disappears. The rounded T_c versus p curve (Figure 2b) near p_c is reminiscent of the quantum critical behavior $T_c \propto |p-p_c|^{1/2}$.[16] However, quantum ferroelectricity appears to be absent in the lowest-temperature region, as the ε peak height in Figure 2a is significantly reduced near p_c, instead of the typical saturation behavior at high ε values. Meanwhile at a pressure of 0.69 GPa, another broad anomaly develops at low temperatures. Applying pressures beyond 0.9 GPa shifts this anomaly to higher temperatures and further diminishes the maximum ε values. The temperature of the anomaly T_m is plotted against pressure in Figure 2b. The broadly rounded ε versus T curves (Figure 2a) are reminiscent of the Bonner–Fisher type susceptibility of an antiferromagnetic linear chain.[17] These facts imply that the development of hidden antiferroelectric correlations might surface and destroy the low-temperature ferroelectric ordering.

Comparison of the crystal structures of [H-55DMBP][Hia] at room temperature (296 K) and at low temperature (50 K) confirms that the ferroelectric transition lowers the symmetry (space group $P\bar{1} \rightarrow P1$) without multiplication of the unit-cell volume (Figure 4). In the low-temperature ferroelectric phase, the protons are localized at either an oxygen or a nitrogen atom; each molecule (A_1, A_2, B_1, or B_2) has an asymmetrically attached proton and, hence, is a monovalent polar ion (Figure 1). The O–H and N^+–H bonds are all aligned in the same direction, and the alternating O–H···N and N^+–H···O^- hydrogen bonds constitute a polar chain (Figure 4a). Since the O–H···N and N^+–H···O^- hydrogen bonds have very similar local environments, they are easily interchangeable by collective proton transfer during polarization reversal between the two degenerate structures.

In the more symmetric room-temperature paraelectric phase, the base molecules B_1 and B_2 are equivalent, and are denoted by B in Figure 4b, and the two acid molecules A_1 and A_2 have inversion symmetry. The number of crystallographically independent hydrogen-bonding sites is also reduced from four (α_1, α_2, β_1, and β_2 in Figure 4a) to two (α and β in Figure 4b). Owing to the inversion symmetry, the acidic hydrogen atoms must be equally allocated on both sides of the acid molecules. If they were locally ordered in O–H···N or N^+–H···O^- hydrogen bonds, then the two nonpolar acid molecules would adopt the neutral H_2ia and divalent ia^{2-} forms, respectively. Otherwise, and more plausibly, the monovalent Hia^- ions could survive on the condition that the protons be equally disordered over the nitrogen- and oxygen-bonded sites, or that they occupy a centered position between the two sites. Although a difference Fourier analysis of the present data yielded nominal hydrogen-atom positions, one centered and the other near a nitrogen atom (Figure 4b), the electron density of the hydrogen atoms, especially when delocalized, is too small to allow an accurate determination of their positions in the presence of the very heavy iodine atoms.

Nevertheless, an alternative means of determining whether the hydrogen atom is localized near either an oxygen or a nitrogen atom is to scrutinize the local π-molecular geometry surrounding the hydrogen bond. It has been shown that the π-electron system is closely coupled with the protonation state of the molecule: deprotonation of the OH group substantially shortens the C–O bond (from 1.32–1.33 to 1.25–1.26 Å) of the haloanilic acids (H_2xa),[18] and protonation of the nitrogen atom widens the C=N–C angle (from 116–117 to 121–123°) of pyridines.[19] The C–O bond lengths and C=N–C bond angles can be obtained with sufficient accuracy to discriminate between the neutral O–H···N and ionic N^+–H···O^- hydrogen bonds. As shown in Figure 4c, the ferroelectric [H-55DMBP][Hia] compound (red circles) reported herein and the antiferroelectric [H-55DMBP][Hca] compound (green squares)[11] undergo very similar structural changes with temperature. The low-temperature phases of both compounds are proton-ordered and consist of the monovalent forms of both molecules linked by

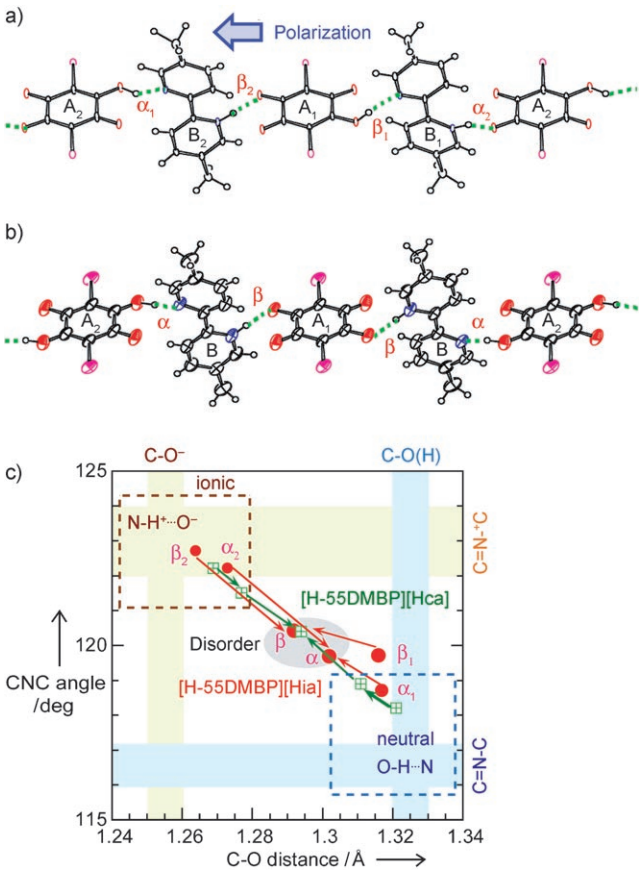

Figure 4. a) The chain of acid (A_1 and A_2) and base (B_1 and B_2) molecules linked by hydrogen bonds (α_1, α_2, β_1, and β_2; dashed lines) in the ferroelectric phase of [H-55DMBP][Hia] at 50 K. C black, H small black, N blue, O red. b) The chain of acid (A_1 and A_2) and base (B) molecules linked by hydrogen bonds (α and β) in the paraelectric phase of [H-55DMBP][Hia] at 296 K. c) Plot of the C=N–C bond angles of the base versus the C–O bond lengths of the acid for the hydrogen-bond sites in [H-55DMBP][Hia] (red circles) at 50 and 296 K ($T_c = 268$ K), and in [H-55DMBP][Hca] (green squares) at 100, 297, and 370 K ($T_c = 318$ K).[11] The arrows indicate the effect of increasing the temperature: the distinct geometries at the sites of the neutral (α_1 and β_1) and ionic (α_2 and β_2) hydrogen bonds in the low-temperature ferroelectric ([H-55DMBP][Hia]) or antiferroelectric ([H-55DMBP][Hca]) phases converge to average geometries at the sites of the disordered (α and β) hydrogen bonds in the paraelectric phases.

typical O–H···N and N^+–H···O^- hydrogen bonds, in agreement with the hydrogen-atom positions determined for [H-55DMBP][Hia] at 50 K. In contrast, the high-temperature paraelectric phases are disordered states containing monovalent molecules, instead of the neutral and divalent molecules. The two hydrogen bonds are each disordered between both tautomeric forms (O–H···N and N^+–H···O^-); the geometrical parameters of the molecules at the two hydrogen-bond sites are similar and are intermediate between those at the four hydrogen-bond sites in the low-temperature phase. According to the maximum entropy method (MEM) analysis recently done on the [H-55DMBP][Hca] salt,[11] the electron density of the proton is distributed in a quasicovalent manner at the middle of O···N bond. An analogous disordered form (containing nominally monovalent molecules) is anticipated for the paraelectric phase of [H-55DMBP][Hia], which has somewhat shorter O···N bonds (2.58, 2.65 Å) than [H-55DMBP][Hca] (2.68 Å).

Thus, the paraelectric–ferroelectric transition in [H-55DMBP][Hca] is related to proton ordering in very strong intermolecular hydrogen bonds, such that the two tautomers O–H···N and N^+–H···O^- are formed. The polarity of the asymmetric molecules can be reversed by a collective proton transfer and the concurrent reorganization of the π-bond geometry. There are several reasons for the acceleration of the proton transfer in this cocrystal. First, the H_2ia molecules contain two π-conjugated fragments corresponding to the enol form of a β-diketone (HO–C=C–C=O; Scheme 1), which are known to participate in strong resonance-assisted hydrogen bonding (RAHB).[20] In the $[Hia]^-$ molecules of [H-55DMBP][Hia], these fragments are linked by short O···O interactions (2.67–2.68 Å). The acid molecules are additionally connected to base molecules through short O···N interactions (2.58–2.65 Å). Since in the resulting bifurcated hydrogen bond, the proton is shared by three surrounding atoms (two oxygen atoms and one nitrogen atom), the potential barrier for proton transfer may be lower than that of a simple O···H···N hydrogen bond. The similarity of the proton affinities of the H_2ia acid and the 55DMBP base is also a probable reason for the proton delocalization, which can further increase the covalent character of the hydrogen bonds.

In summary, the polarity of supramolecular chains consisting of alternating monoprotonated π-molecular acid and base molecules can be successfully reversed through cooperative proton dynamics in response to a small applied electric field. The process exchanges two hydrogen-bond tautomers O–H···N and N^+–H···O^-, and concomitantly rearranges the geometries of both π molecules, giving rise to a large spontaneous polarization and dielectric constant. The new compound [H-55DMBP][Hia] may be considered as a first representative of what could become a large class of supramolecular ferroelectrics.

Received: January 30, 2007
Published online: March 30, 2007

Keywords: dielectric properties · ferroelectricity · hydrogen bonds · hydrogen transfer · supramolecular chemistry

[1] a) G. A. Jeffery, *An Introduction to Hydrogen Bonding*, Oxford University Press, Oxford, **1997**; b) J.-M. Lehn, *Supramolecular Chemistry: Concepts and Perspectives*, Wiley-VCH, Weinheim, **1995**; c) G. R. Desiraju, *Crystal Engineering: The Design of Organic Solids*, Elsevier, Amsterdam, **1989**.
[2] *Proton Transfer in Hydrogen-Bonded Systems* (Ed.: T. Bountis), Plenum, New York, **1992**.
[3] T. Mitani, T. Inabe in *Spectroscopy of New Materials* (Eds.: R. J. H. Clark, R. E. Hester), Wiley, New York, **1993**, pp. 291–331.
[4] T. Sugawara, I. Takasu, *Adv. Phys. Org. Chem.* **1999**, *32*, 219–265.
[5] E. J. Samuelsen, D. Semmingsen, *J. Phys. Chem. Solids* **1977**, *38*, 1275–1283.

[6] M. E. Lines, A. M. Glass, *Principles and Applications of Ferroelectrics and Related Materials*, Oxford University Press, New York, **1977**.
[7] M. Szafrański, A. Katrusiak, G. J. McIntyre, *Phys. Rev. Lett.* **2002**, *89*, 215507.
[8] a) T. Steiner, I. Majerz, C. C. Wilson, *Angew. Chem.* **2001**, *113*, 2728 – 2731; *Angew. Chem. Int. Ed.* **2001**, *40*, 2651 – 2654; b) J. A. Cowan, J. A. K. Howard, G. J. McIntyre, S. M.-F. Lo, I. D. Williams, *Acta Crystallogr. Sect. B* **2003**, *59*, 794 – 801; c) A. Parkin, S. M. Harte, A. E. Goeta, C. C. Wilson, *New J. Chem.* **2004**, *28*, 718 – 721.
[9] T. Steiner, *Angew. Chem.* **2002**, *114*, 50 – 80; *Angew. Chem. Int. Ed.* **2002**, *41*, 48 – 76.
[10] a) S. Horiuchi, F. Ishii, R. Kumai, Y. Okimoto, H. Tachibana, N. Nagaosa, Y. Tokura, *Nat. Mater.* **2005**, *4*, 163 – 166; b) S. Horiuchi, R. Kumai, Y. Tokura, *J. Am. Chem. Soc.* **2005**, *127*, 5010 – 5011.
[11] R. Kumai, S. Horiuchi, Y. Okimoto, Y. Tokura, *J. Chem. Phys.* **2006**, *125*, 084715.
[12] Crystallographic data for [H-55DMBP][Hia]: For the paraelectric phase (296 K): $C_{18}H_{14}I_2N_2O_4$, $M_r = 576.13$, triclinic, space group $P\bar{1}$ (no. 2), $a = 8.7726(16)$, $b = 10.0724(18)$, $c = 12.748(2)$ Å, $\alpha = 67.390(8)$, $\beta = 66.94(1)$, $\gamma = 66.704(6)°$, $V = 916.1(3)$ Å^3, $Z = 2$, $\rho_{calcd} = 2.088$ g cm^{-3}, $R_{int} = 0.009$, $R = 0.030$, $wR = 0.046$, GOF = 0.954, 292 parameters, 6629 reflections ($I > 2\sigma(I)$), $2\theta < 90.5°$. For the ferroelectric phase (50 K): $C_{18}H_{14}I_2N_2O_4$, $M_r = 576.13$, triclinic, space group $P1$ (no. 1), $a = 8.7253(4)$, $b = 9.9993(7)$, $c = 12.6399(5)$ Å, $\alpha = 67.502(4)$, $\beta = 66.561(2)$, $\gamma = 66.452(3)°$, $V = 894.12(8)$ Å^3, $Z = 2$, $\rho_{calcd} = 2.140$ g cm^{-3}, $R_{int} = 0.030$, $R = 0.037$, $wR = 0.046$, GOF = 0.994, 547 parameters, 17800 reflections ($I > 2\sigma(I)$), $2\theta < 90.5°$. The data collections were performed with silicon-monochromated synchrotron radiation ($\lambda = 0.688$ Å, beam size: 0.3×0.7 mm^2) by using a Rigaku DSC imaging-plate system and a helium-gas refrigerator at beamline BL-1A of the Photon Factory (PF), High-Energy Accelerator Research Organization (KEK). The monochromated beam was focused by a bent cylindrical mirror made from a silicon crystal coated with rhodium. The RapidAUTO program (Rigaku) was used for the two-dimensional image processing. After solving the structure with direct methods by using the program Sir2002, the non-hydrogen atoms were refined with anisotropic thermal factors using the CrystalStructure software package (MSC). CCDC-635129 (296 K) and CCDC-635130 (50 K) contain the supplementary crystallographic data for this paper. These data can be obtained free of charge from The Cambridge Crystallographic Data Centre via www.ccdc.cam.ac.uk/data_request/cif.
[13] R. Blinc, *J. Phys. Chem. Solids* **1960**, *13*, 204 – 211.
[14] K. Murata, H. Yoshino, H. O. Yadav, Y. Honda, N. Shirakawa, *Rev. Sci. Instrum.* **1997**, *68*, 2490 – 2493.
[15] G. A. Samara, T. Sakudo, K. Yoshimitsu, *Phys. Rev. Lett.* **1975**, *35*, 1767 – 1769.
[16] T. Schneider, H. Beck, E. Stoll, *Phys. Rev. B* **1976**, *13*, 1123 – 1130.
[17] J. C. Bonner, M. E. Fisher, *Phys. Rev.* **1964**, *135*, A640 – 658.
[18] a) C. Robl, G. M. Sheldrick, *Z. Kristallogr.* **1988**, *184*, 295 – 300; b) E. K. Andersen, *Acta Cryst.* **1967**, *22*, 196 – 201; c) H. Ishida, S. Kashino, *Acta Crystallogr. Sect. C* **1999**, *55*, 1149 – 1152.
[19] I. Majerz, A. Koll, *Acta Crystallogr. Sect. B* **2004**, *60*, 406 – 415.
[20] G. Gilli, F. Bellucci, V. Ferretti, V. Bertolasi, *J. Am. Chem. Soc.* **1989**, *111*, 1023 – 1028.

